

Jason N. Itri, Andrew M. Vosko, Analyne Schroeder, Joanna M. Dragich, Stephan Michel and Christopher S. Colwell

J Neurophysiol 103:632-640, 2010. First published Nov 25, 2009; doi:10.1152/jn.00670.2009

You might find this additional information useful...

This article cites 58 articles, 29 of which you can access free at:

<http://jn.physiology.org/cgi/content/full/103/2/632#BIBL>

Updated information and services including high-resolution figures, can be found at:

<http://jn.physiology.org/cgi/content/full/103/2/632>

Additional material and information about *Journal of Neurophysiology* can be found at:

<http://www.the-aps.org/publications/jn>

This information is current as of February 6, 2010 .

Circadian Regulation of A-Type Potassium Currents in the Suprachiasmatic Nucleus

Jason N. Itri, Andrew M. Vosko, Analyne Schroeder, Joanna M. Dragich, Stephan Michel, and Christopher S. Colwell

Department of Psychiatry and Biobehavioral Sciences, University of California, Los Angeles, California

Submitted 28 July 2009; accepted in final form 23 November 2009

Itri JN, Vosko AM, Schroeder A, Dragich JM, Michel S, Colwell CS. Circadian regulation of A-type potassium currents in the suprachiasmatic nucleus. *J Neurophysiol* 103: 632–640, 2010. First published November 25, 2009; doi:10.1152/jn.00670.2009. In mammals, the precise circadian timing of many biological processes depends on the generation of oscillations in neural activity of pacemaker cells in the suprachiasmatic nucleus (SCN) of the hypothalamus. Understanding the ionic mechanisms underlying these rhythms is an important goal of research in chronobiology. Previous work has shown that SCN neurons express A-type potassium currents (IAs), but little is known about the properties of this current in the SCN. We sought to characterize some of these properties, including the identities of IA channel subunits found in the SCN and the circadian regulation of IA itself. In this study, we were able to detect significant hybridization for *Shal*-related family members 1 and 2 (Kv4.1 and 4.2) within the SCN. In addition, we used Western blot to show that the Kv4.1 and 4.2 proteins are expressed in SCN tissue. We further show that the magnitude of the IA current exhibits a diurnal rhythm that peaks during the day in the dorsal region of the mouse SCN. This rhythm seems to be driven by a subset of SCN neurons with a larger peak current and a longer decay constant. Importantly, this rhythm in neurons in the dorsal SCN continues in constant darkness, providing an important demonstration of the circadian regulation of an intrinsic voltage-gated current in mammalian cells. We conclude that the anatomical expression, biophysical properties, and pharmacological profiles measured are all consistent with the SCN IA current being generated by Kv4 channels. Additionally, these data suggest a role for IA in the regulation of spontaneous action potential firing during the transitions between day/night and in the integration of synaptic inputs to SCN neurons throughout the daily cycle.

INTRODUCTION

Daily biological rhythms are endogenously generated, regulated, and synchronized by networks of circadian oscillators communicating throughout the brain and periphery. In mammals, the suprachiasmatic nucleus (SCN) of the hypothalamus contains the “master” oscillatory network necessary for coordinating these rhythms. A unique property of mammalian SCN neurons and one essential to the function of the circadian timing system is the ability to generate intrinsic circadian rhythms in electrical activity (Schwartz et al. 1987; Yamaguchi et al. 2003). The SCN has been shown to generate neural activity rhythms in isolation from the rest of the organism with both the brain slice preparation (Schaap et al. 2003) and in cultures made from SCN tissue (Herzog et al. 1998; Honma et al. 1998; Welsh et al. 1995). These studies are consistent with

the idea that many SCN neurons are stable, self-sustained oscillators that have the intrinsic capacity to generate circadian rhythms in electrical activity.

Neurons within the SCN also generate robust, synchronized rhythms in the transcription, translation, and degradation of key “clock genes” in an autoregulatory loop that has an endogenous periodicity of ~24 h (Ko and Takahashi 2006; Reppert and Weaver 2002). This autoregulatory feedback loop is necessary for both circadian rhythms in electrical activity and behavior (Albus et al. 2002). Although other mammalian cell populations also can generate these rhythms in gene expression, we do not yet understand how this molecular feedback loop interacts with intrinsic membrane currents to produce the self-sustained, physiological rhythms in electrical activity found in the SCN. We believe that this is a critical gap in our knowledge of the SCN and the mammalian circadian system.

Voltage-dependent potassium (K⁺) currents are critical regulators of membrane excitability in neurons (Rudy 1988) and are likely candidates for coupling the putative molecular clock to spontaneous firing rate rhythms in SCN neurons. Previous studies in the SCN have characterized a number of intrinsic voltage-gated K⁺ currents that are likely to play important roles in regulating spontaneous firing rate (reviewed by Ko et al. 2009; Kuhlman and McMahon 2006; Schaap et al. 2003). In other neurons, the subthreshold-operating A-type K⁺ current (IA) is largely involved in the regulation of neuronal excitability and the timing of action potential firing. Within the SCN, this current has been described and proposed as a likely candidate to regulate spontaneous firing rate (Alvado and Allen 2008; Bouskila and Dudek 1995; Huang 1993). Before any definitive roles can be credited to IA in the SCN, however, some key features, such as the channel subunits responsible for this current and the rhythmic properties of IA in the SCN, must first be examined.

To better understand the roles of IA in the SCN, we first sought to determine the expression patterns of *Shal*-type K⁺ channels that are largely responsible for the IA current in other brain regions (Birnbaum et al. 2004; Jerng et al. 2004). Next, we used whole cell patch electrophysiological techniques to record and characterize these currents in mouse SCN neurons. We specifically sought to determine whether the magnitude or voltage dependence of these currents varied with a diurnal or circadian rhythm. Furthermore, because the SCN is a heterogeneous structure made up of anatomically and functionally distinct subdivisions (Antle and Silver 2005; Morin 2007), we examined possible regional differences in these currents. Together, these experiments comprehensively examine the prop-

Address for reprint requests and other correspondence: C. S. Colwell, Dept. of Psychiatry, Univ. of California–Los Angeles, 760 Westwood Plaza, Los Angeles, CA 90024-1759 (E-mail: ccolwell@mednet.ucla.edu).

erties of the IA in SCN neurons and provide a framework by which this current contributes to the physiological properties of the SCN circuit.

METHODS

Experimental animals

Our studies used 4- to 8-wk-old male C57BL/6J mice. All mice were housed in cages within light-tight chambers with controlled lighting conditions. The experimental protocols used in this study were approved by the University of California, Los Angeles (UCLA) Animal Research Committee and all recommendations for animal use and welfare, as dictated by the UCLA Division of Laboratory Animals and the guidelines from the National Institutes of Health, were followed.

Behavioral analysis

Male mice were housed individually, and their wheel-running activity was recorded as previously described (Colwell et al. 2003, 2004). The running wheels and data acquisition system were obtained from Mini Mitter (Bend, OR). Mice were exposed to a 12:12 light/dark (LD) cycle for at least 1 wk (light intensity ~500 lux). Zeitgeber time (ZT) is used to describe the projected time of the circadian clock within the SCN based on the previous light cycle, with lights-on defined as ZT 0. Animals were killed between ZT 3–4 in the LD cycle for recording during the day and ZT 11.5 for recording during the night. Some mice were placed into constant darkness (DD) for 7–10 days to assess their free-running activity pattern. Circadian time (CT) was determined by activity records with activity onset denoted as CT12. Animals were removed during the appropriate phase and anesthetized in complete darkness using infrared viewers. Animals were killed between CT 3–4 in the DD cycle for recording during subjective day and CT 12–13 for recording during the subjective night.

Riboprobe synthesis

A 370-bp riboprobe designed to hybridize with nucleotides 1,484–1,854 of mouse *Kcnd1* (NM_008423.1) was generated by PCR amplification from adult mouse brain cDNA using primers Kv4.1f3 (5'-acagactaactttcagtgaggc-3') and Kv4.1r3 (5'-actaggggaggaaggtgact-3'), as they had been used for mapping *Kcnd1* in the Allen Brain Atlas (www.brain-map.org). The PCR product was subcloned into a pCR-BLUNT II-TOPO vector (TOPO Blunt cloning kit, Invitrogen, Carlsbad, CA) and confirmed by sequencing. Plasmids were digested with either *HindIII* or *XbaI* followed by phenol/chloroform extraction and isopropanol precipitation to yield antisense and sense templates for in vitro transcription.

A 680-bp riboprobe designed to hybridize with nucleotides 1,337–2,017 of mouse *Kcnd2* (NM_019697) was generated by PCR amplification from adult mouse brain cDNA using primers Kv4.2F (5'-gggaagattttgggtccat-3') and Kv4.2R (5'-tctggggtggttactggag-3'). The PCR product was subcloned into a pCR2.1-TOPO vector (TOPO TA cloning kit, Invitrogen) and confirmed by sequencing. Plasmids were digested with either *HindIII* or *NotI*, followed by a phenol/chloroform extraction and isopropanol precipitation to yield antisense and sense templates for in vitro transcription.

Both riboprobes were synthesized from 1 μ g of template cDNA in a reaction mixture containing 100 μ Ci of UTP 35 S (1,250 Ci/mmol, Perkin Elmer, Wellesley, MA), 5 \times transcription buffer (Promega, Madison, WI), 0.1 M dithiothreitol (DTT, Promega), 10 mM of each rATP, rCTP, and rGTP, 40U RNase inhibitor, and the appropriate RNA transcriptase (SP6 or T7) for 3 h at 37°C. Unincorporated nucleotides were removed using RNase-free microspin columns

(Bio-Spin 30, Biorad, Hercules, CA), and probe yields were calculated by scintillation counting.

In situ hybridization

In situ hybridization (ISH) on tissue sections containing the SCN was done using previously described procedures (Chaudhury et al. 2008; Wang et al. 2009). Brains were removed, immediately frozen in embedding media (OTC, Sakura Finetek), and stored at -80°C . Coronal sections were taken at 20 μm and mounted onto superfrost plus slides (Fisher Scientific, Pittsburgh, PA). On day 1, slides were warmed to room temperature, briefly washed in PBS and fixed in 4% paraformaldehyde, air-dried, blocked by acetylation with acetic anhydride, and dehydrated. After air drying, slides were placed in prehybridization buffer (50% formamide, 3 M NaCl, 20 mM EDTA, 400 mM Tris, pH 7.8, 0.4% SDS, 2 \times Denhardt's, 500 mg/ml tRNA, and 50 mg/ml polyA RNA) for 1 h at 55°C. Sections were hybridized overnight at 55°C in humidified chambers in hybridization buffer (50% formamide, 10% dextran sulfate, 3 M NaCl, 20 mM EDTA, 400 mM Tris, pH 7.8, 0.4% SDS, 2 \times Denhardt's, 500 mg/ml tRNA, and 50 mg/ml polyA RNA, 40 mM DTT), where each slide was incubated with 1–4 million cpm/70 ml of riboprobe. After hybridization, the slides were washed for 15 min in 4 \times SSC at 55°C, in 2 \times SSC for 1 h at room temperature, and in RNase A (20 $\mu\text{g}/\text{ml}$) treated at 37°C for 30 min to remove unbound probe. To further reduce nonspecific hybridization, the slides were washed twice in 2 \times SSC at 37°C and for 1 h in 0.1 \times SSC at 62–67°C. All posthybridization washes contained 1 mM sodium thiosulfate, except in the RNase A and ethanol washes. Slides were serially dehydrated in ethanol containing 0.3 M ammonium acetate and exposed to Kodak Biomax MR film (Kodak, Rochester, NY) along with a ^{14}C slide standard (American Radiolabeled Chemicals, St. Louis, MO). The slides were counterstained with cresyl violet to serve as a reference. Densitometric analysis of hybridization intensity was done as described using National Institutes of Health image software (Chaudhury et al. 2008; Wang et al. 2009).

Western blot analysis

Western blots were performed using previously described procedures (Choi et al. 2008; Wang et al. 2009). Whole SCN from three to four mice were pooled together and flash frozen in 500 μl of ice-cold homogenization buffer (50 mM Tris-HCl, 50 mM NaF, 10 mM EGTA, 10 mM EDTA, 80 μM sodium molybdate, 5 mM sodium pyrophosphate, 1 mM sodium orthovanadate, 0.01% Triton X-100, and 4 mM para-nitrophenylphosphate). The homogenization buffer also contained cocktails of protease inhibitors (Protease Inhibitors Complete, Roche Molecular Biochemicals, Indianapolis, IN) and protein phosphatase inhibitors (Protein Phosphatase Inhibitor Cocktail I and II, Sigma-Aldrich, St. Louis, MO). The tissue was homogenized with an ultrasonic cell disruptor (3 times for 5 s). Immediately after homogenization, aliquots were removed to measure protein concentration using a Bio-Rad Protein Assay Kit (Hercules, CA). Equal amounts of denaturing protein loading buffer [0.5 M Tris-HCl, pH 6.8, 4.4% (wt/vol) SDS, 20% (vol/vol) glycerol, 2% 2-mercaptoethanol, and bromophenol blue] were added to the remaining homogenates and heated to 100°C for 5 min. Homogenates containing 30 μg of protein each were electrophoresed on 15% SDS-PAGE gels, transferred to nitrocellulose membranes, blocked with 2% milk, and probed with primary antisera overnight [Kv4.1 (1:400) and Kv4.2 (1:200), Alomone Labs, Jerusalem, Israel]. The membranes were incubated with horseradish peroxidase-conjugated anti-mouse or anti-rabbit secondary IgG (1:1,000), and protein signals were visualized by chemiluminescence (Immun-Star HRP detection kit, Bio-Rad). A phosphorimager was used for quantification, and day/night comparisons were analyzed simultaneously, using identical settings. Protein bands were boxed, and the integrated intensity of all the pixels

within that band was calculated above object average background levels of a box of the same size. To control for potential variations in loading, the optical density of bands for each protein of interest were normalized to the optical density values obtained for tubulin loading control bands in each lane. Tubulin optical density values did not vary as a function of time (ZT 6: $1,330 \pm 64$; ZT 14: $1,293 \pm 21$). Day/night normalized density values were analyzed for significance using Student's *t*-test ($n = 3$).

Brain slice preparation

Brain slices were prepared using standard techniques (Colwell 2000, 2001) using mice between 4 and 8 wk of age. Animals received anesthesia and were killed by decapitation, and brains were dissected and placed in cold, oxygenated artificial cerebral spinal fluid (ACSF) containing (in mM) 130 NaCl, 26 NaHCO₃, 3 KCl, 5 MgCl₂, 1.25 NaH₂PO₄, 1.0 CaCl₂, and 10 glucose (pH 7.2–7.4). After cutting slices (DSK Model 1500E, Microslicer, Kyato, Japan) from areas to be analyzed, coronal sections were placed in ACSF (25–27°C) for ≥ 1 h (in this solution, CaCl₂ is increased to 2 mM and MgCl₂ is decreased to 2 mM). Slices were constantly oxygenated with 95% O₂-5% CO₂ (pH 7.2–7.4, osmolality 290–300 mOsm).

Whole cell patch-clamp electrophysiology

Methods were similar to those described previously (Itri et al. 2005; Michel et al. 2006). Briefly, slices were placed in a recording chamber (PH-1, Warner Instruments, Hamden, CT) attached to the stage of a fixed-stage upright microscope. The standard solution in the patch pipette contained (in mM): 112.5 K-gluconate, 1 EGTA, 10 HEPES, 5 MgATP, 1 GTP, 0.1 leupeptin, 10 phosphocreatine, 4 NaCl, 17.5 KCl, 0.5 CaCl₂, and 1 MgCl₂. The pH was adjusted to 7.25–7.3 and the osmolality to between 290 and 300 mOsm. Whole cell recordings were obtained with an Axon Instruments 200B amplifier and monitored on-line with pCLAMP (Ver. 8.0, Molecular Devices, Sunnyvale, CA). Data were not collected if access resistance was >40 M Ω or if the value changed significantly ($>20\%$) during the course of the experiment. In these studies, we used a 70% compensation using positive feedback correction. The junction potentials between the pipette and the extracellular solution was cancelled by the voltage-offset of the amplifier before establishing a seal and was not further corrected. The standard extracellular solution used for all experiments was ACSF. Drug treatments were performed by dissolving pharmacological agents in the ACSF used to bathe the slices during recording. Solution exchanges within the slice were achieved by a rapid gravity feed delivery system. In our system, the effects of bath applied drugs began within 15 s and were typically maximal by 3–5 min.

Currents were recorded with pClamp using the voltage-clamp recording configuration, then analyzed using ClampFit (9.0) and Minianalysis software (Ver. 5.2.12, Synaptosoft, Decatur, GA). To isolate IA currents in SCN neurons, two voltage-step protocols were used in the whole cell patch-clamp configuration. The first protocol consisted of a 100-ms prepulse at -90 mV (to elicit maximal conductance) followed by a 250-ms step at progressively depolarized potentials (-80 to 50 mV, 5-mV steps). The second protocol consisted of a 100-ms prepulse at -50 mV (to remove the contribution of the IA current) followed by a 250-ms step at progressively depolarized potentials (-80 to 50 mV, 5-mV steps). Current traces from the second protocol were subtracted from the first to isolate IA currents. Activation curves were generated using data collected from the isolated IA currents, whereas inactivation curves were generated by using the following protocol in the whole cell voltage-clamp configuration: 100-ms prepulses of varying potentials (-100 to -30 mV, 5-mV steps) followed by a 250-ms step at $+50$ mV to elicit maximal current. The ACSF perfusion solution contained bicuculline (25 μ M) to block GABA_A-mediated currents, TTX (0.5 μ M) to block fast voltage-activated sodium channels, and cadmium (25 μ M) to block

voltage-activated calcium channels. The intracellular solution also contained 1,2-bis(o-aminophenoxy)ethane-*N,N,N',N'*-tetraacetic acid (BAPTA, 1 mM) to buffer intracellular calcium and inhibit calcium-dependent potassium currents.

Statistical measurements

Possible significant differences between control and experimental groups were generally determined by *t*-tests or Mann-Whitney rank sum tests when appropriate. Values were considered significantly different if $P < 0.05$. All tests were performed using SigmaStat (version 3.5). In the text, values are shown as means \pm SE. Each group of data are collected from at least three animals, with n representing the number of cells recorded.

RESULTS

Kv4.1 and Kv4.2 message is expressed in the SCN

The *Shal*-related family of K⁺ channels is thought to be largely responsible for generation of the IA current (Isbrandt et al. 2000; Jerng et al. 2004; Maffie and Rudy 2008). To determine whether these genes are expressed in the SCN, we used ISH to measure *Kv4.1* and *Kv4.2* message in the mouse SCN. Expression of transcripts for *Kv4.1* and *Kv4.2* was observed throughout the SCN (Fig. 1, *A* and *B*). The sense probes did not exhibit labeling in the SCN under identical hybridization conditions (Fig. 1*C*). Both transcripts also showed expression in the periventricular hypothalamus, habenula, hippocampus, and cortex, and the *Kv4.2* transcript showed stronger labeling in the striatum. Analysis of the OD measurements of *Kv* expression (normalized to background) indicated that the levels of expression were not significantly different in the SCN between day (ZT 2–6) and night (ZT 12–16). For *Kv4.1*, the average OD measurements in the day were 0.47 ± 0.08 ($n = 3$) and 0.32 ± 0.11 ($n = 3$) in the night (*t*-test; $P = 0.34$). For *Kv4.2*, the average OD measurements in the day were 0.36 ± 0.05 ($n = 4$) and 0.38 ± 0.12 ($n = 4$) in the night (*t*-test; $P = 0.84$). For comparison, in the SCN, the mean OD of *Per2* was higher at day (ZT 6: 1.75 ± 0.32 OD, $n = 3$) than in the night (ZT 16: 0.85 ± 0.14 OD, $n = 3$; *t*-test, $P < 0.05$).

Kv4.1 and Kv4.2 protein is expressed in the SCN

To determine whether *Kv4.1* and *Kv4.2* proteins were expressed in the SCN, we measured protein levels from the SCN of mice using Western blots (Fig. 2*A*). Total protein expression was normalized to tubulin, which does not vary as a function of time of day (see METHODS). The *Kv* protein bands were not detected in controls in which the *Kv4.1* and 4.2 primary antibodies were preabsorbed or omitted (data not shown). Consistent with our ISH data, we found that both *Kv4.1* and *Kv4.2* were expressed in the SCN and that levels of expression did not vary significantly as a function of time of day (Fig. 2*B*). The average OD measurements of *Kv4.1* (normalized to loading controls) in the day (ZT 6) was 0.13 ± 0.03 ($n = 3$) and 0.14 ± 0.02 ($n = 3$) in the night (ZT 14; *t*-test; $P = 0.79$). Similarly, the OD average measurements of *Kv4.2* (normalized to loading controls) in the day was 0.36 ± 0.14 ($n = 3$) and 0.47 ± 0.18 ($n = 3$) in the night (Mann-Whitney rank sum test; $P = 0.70$). For comparison, these same methods did detect a significant daily rhythm in *PER2* expression. For example, OD

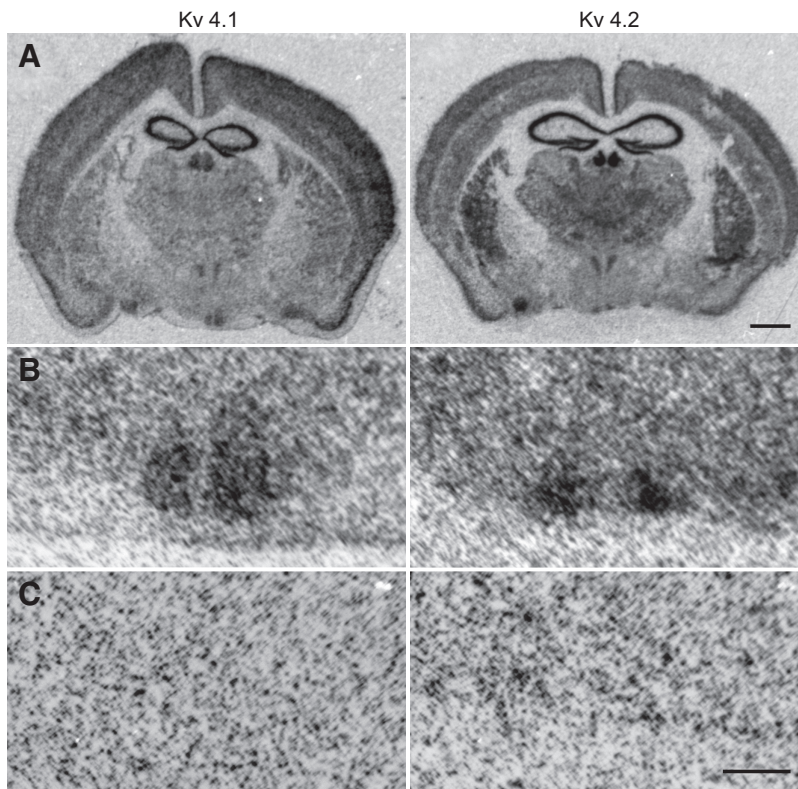


FIG. 1. In situ hybridization shows expression of the mRNA for *Kv4.1* (*kcmd1*) and *Kv4.2* (*kcmd2*) in the mouse suprachiasmatic nucleus (SCN). *A*: autoradiogram images ($\times 100$) of hybridization with antisense probes. Scale bar, 1 mm. *B*: autoradiogram images ($\times 400$) from hybridization with antisense probes. *C*: autoradiogram images ($\times 400$) from hybridization with sense probes. Scale bar, 200 μm .

measurements of PER2 (normalized to loading controls) during the day was 0.25 ± 0.05 compared with 0.12 ± 0.02 at the trough ($n = 3$; t -test, $P < 0.05$).

Characterization of IA currents

We used the whole cell voltage-clamp technique to isolate and record IA currents from neurons in the mouse SCN (Fig. 3). The ACSF perfusion solution contained bicuculline (25 μM), TTX (0.5 μM), and cadmium (25 μM). The intracellular solution contained BAPTA (1 mM). Voltage-dependent activation of IA was measured from the isolated currents (Fig. 3C). Outward currents with IA inactivated (Fig. 3B, prepulse of -50 mV) were subtracted from current responses elicited from -90 mV, which removes inactivation of IA and allows for maximum IA

current (Fig. 3A). The voltage dependence of the inactivation was determined from current responses to a depolarizing pulse ($+50$ mV) after prepulses to different holding potentials (see METHODS for details). For both protocols, each prepulse sweep was followed by a 500-ms pause at -90 mV to ensure that the channels had recovered from inactivation by the start of the following sweep. The overlap of inactivation and activation curves (Fig. 3D) suggests that IA currents are active between -60 and -40 mV. IA currents were detected in every SCN neuron ($n = 169$) in both dorsal and ventral regions, although the amplitude and kinetic parameters varied by region and phase. Each of these cells was determined to be within the SCN by directly visualizing the cell's location with IR-DIC videomicroscopy before any data were collected.

To determine the sensitivity of IA currents to 4-aminopyridine (4-AP), we applied a -90 -mV prepulse (100 ms) followed by a $+50$ -mV pulse (900 ms) in the whole cell voltage-clamp configuration to elicit maximal IA current (Fig. 4A). Bath applied 4-AP reversibly blocked IA currents in SCN neurons in a dose-dependent manner, with 5 mM 4-AP blocking $\sim 85\%$ of the total IA current (Fig. 4B). In contrast, bathing the neurons in concentrations of tetraethylammonium (TEA) ranging from 0.1 to 10 mM failed to have any measurable effect on IA currents measured in SCN neurons (Fig. 4C).

Magnitude of IA currents varies with circadian cycle

The IA current traces were used to generate I - V relationships for IA currents in the dorsal and ventral regions of the SCN, during both day and night. Under an LD cycle, there was a significant increase (ANOVA, $P < 0.01$) in the magnitude of IA currents in the dSCN during the day (ZT 4–6, $n = 27$) compared with the night (ZT 13–16, $n = 25$; Fig. 5A). To

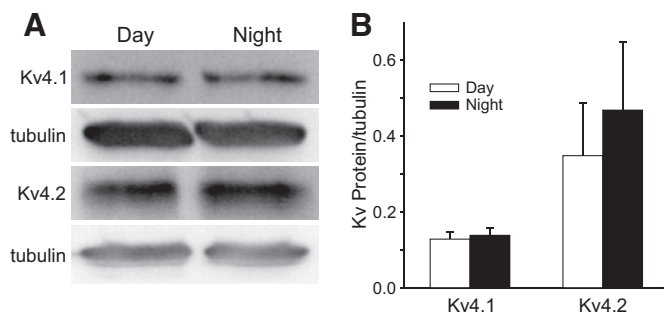


FIG. 2. Kv4 channel proteins are expressed in the mouse SCN. Western blots were used to measure levels of Kv4.1 and Kv4.2. *A*: examples of the blots and (*B*) histograms of chemiluminescent signal normalized to tubulin. SCN tissue was collected from mice during the day [Zeitgeber time (ZT) 6] and during the night (ZT 14). We did not see any significant difference in expression between these 2 time points. In this and other figures, values are shown as means \pm SE.

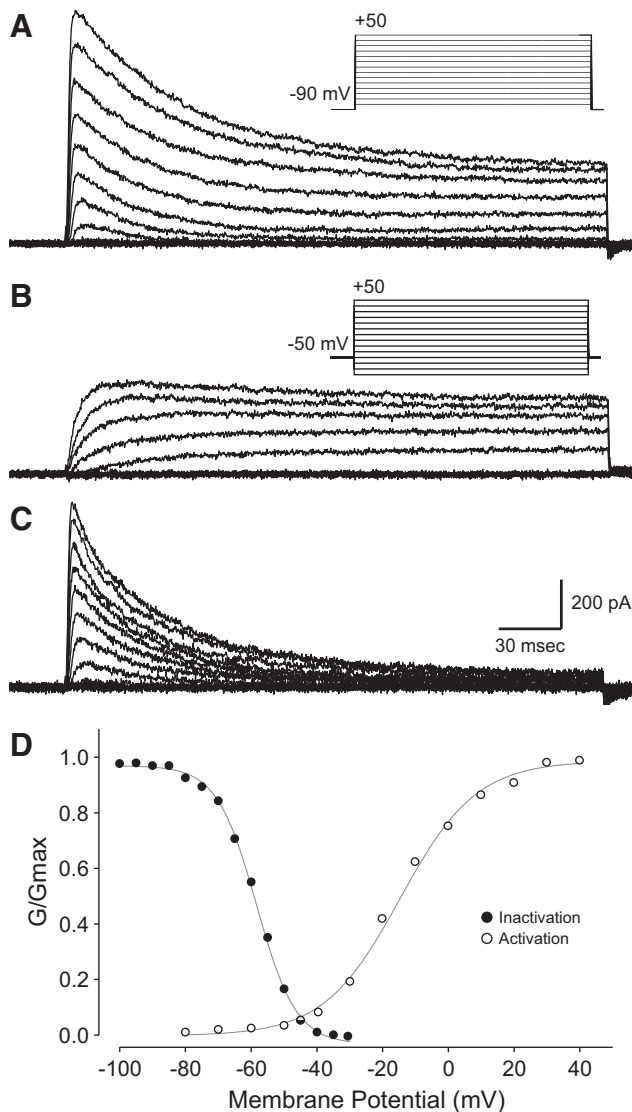


FIG. 3. Isolation of A-type potassium currents (IA) currents in SCN neurons. **A:** current traces elicited by progressively depolarizing voltage pulses (-80 to +50 mV) after a -90-mV prepulse (100 ms) to remove inactivation of IA and obtain maximal IA currents. **B:** prepulses of -50 mV were used to inactivate IA, and current responses were recorded with the otherwise identical protocol as in **A**. **C:** isolated IA current obtained by subtracting traces lacking IA (**B**) from current responses with maximal IA (**A**). **D:** inactivation curve (●) was constructed from current responses to a depolarizing pulse (+50 mV) after prepulses to different holding potentials. Inactivation and activation (○) curves show some overlap between -60 and -40 mV. The data points are plotted every 10 mV even though 5-mV steps were performed. One extra data point is plotted at -45 mV showing a visible conductance in both inactivation and activation curves.

determine whether the observed daily rhythm in IA currents was circadian, we measured IA currents in dorsal SCN neurons from animals housed in DD (Fig. 5B). Wheel-running activity was used to determine the phase of the daily cycle. We found the same relationship in the magnitude of IA currents in the dorsal SCN between subjective day (CT 4–8, $n = 12$) and early subjective night (CT 13–16, $n = 10$), confirming that the rhythm is indeed circadian. In the ventral SCN, there was no significant day/night difference (ANOVA, $P = 0.80$), although IA currents measured during the day ($n = 13$) in this region

were slightly larger in amplitude compared with those measured during the night ($n = 13$, Fig. 5C).

We carried out further analysis of the IA currents in the dSCN region to better understand their diurnal and circadian regulation. Examples of largest magnitude IA currents recorded in day and night show this difference (Fig. 6, A and B). Activation curves were compared for dorsal SCN (dSCN) neurons during the day (midpoint V -16.7 ± 0.7 mV, slope factor $k = 9.7 \pm 0.6$ mV, $n = 10$) and night (midpoint V -14.9 ± 1.1 mV, slope factor $k = 11.9 \pm 1.0$ mV, $n = 12$), but there were no significant differences in the voltage dependence of IA activation (Fig. 6C). Analysis of peak amplitude indicates that subsets of cells with large amplitude currents are responsible for the peak during the day (Fig. 6D). SCN neurons were sorted into 100-pA amplitude bins and plotted according to the number of neurons in each bin. The distribution of IA currents measured in the dorsal SCN during the night peaked between 100 and 400 pA, with a majority of neurons falling within this range. In contrast, dorsal SCN neurons recorded during the day showed one peak in amplitude distribution between 300 and 400 pA and another significant peak between 600 and 800 pA. Finally, we separated all dorsal SCN neurons into small-amplitude (<400 pA) and large-amplitude (>400 pA) groups and compared the decay constant (τ) for each

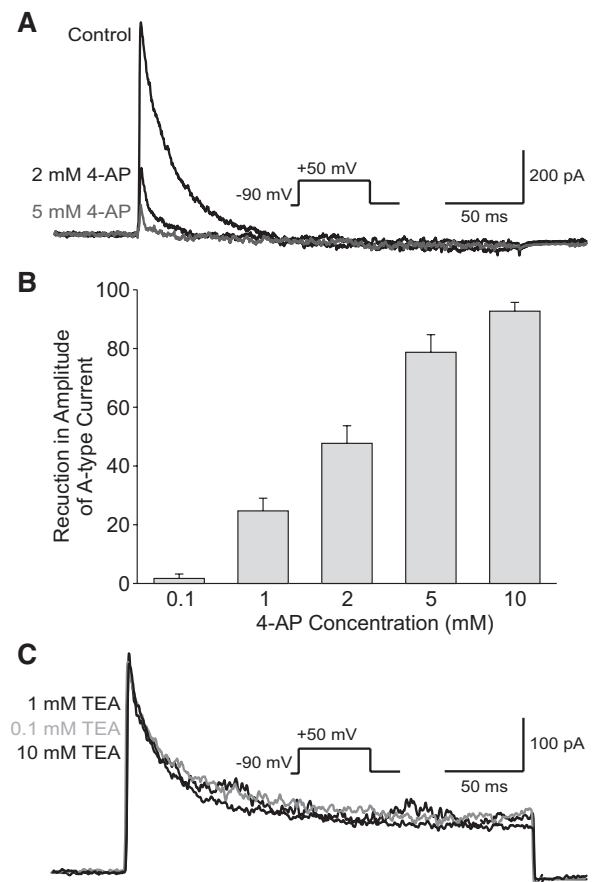


FIG. 4. Pharmacological characterization of IA currents in SCN neurons. **A:** IA currents in dorsal SCN neurons recorded during the day using the isolation protocol described above. Examples are shown to indicate that IA was sensitive to bath application of 4-AP (>1 mM). **B:** effects of 4-AP on IA currents measured at 50 mV were concentration dependent, with 50% blockade occurring at 2 mM. **C:** bath application of tetraethylammonium (TEA; 0.1–10 mM) was without effect on the magnitude of the IA current.

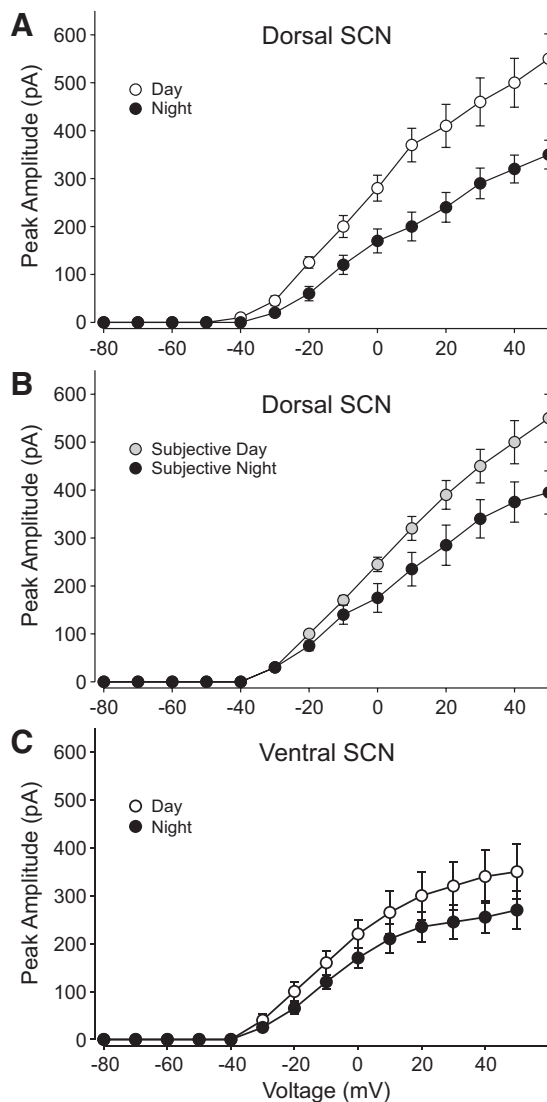


FIG. 5. The magnitude of the IA in dorsal SCN neurons exhibited a circadian rhythm. *A*: IA currents recorded in the dorsal SCN during the day (○) were significantly greater than during the night (●). *B*: This diurnal difference continued when mice were held in constant darkness when running activity was used to assess subjective day (○) and night (●). Activity onset is defined as CT 12. *C*: IA currents recorded in the vSCN during the day were not significantly different from during the night. Each current-voltage relationship consists of data collected from 10 to 17 neurons. Markers and error bars represent means \pm SE.

group. During the day, τ was significantly shorter for IA currents in the small-amplitude group ($\tau = 15.8$ ms, $n = 6$) compared with the large-amplitude group ($\tau = 21.5$ ms, $n = 10$; t -test, $P < 0.05$). During the night, τ was significantly shorter for IA currents in the small-amplitude group ($\tau = 16.1$ ms, $n = 15$) compared with both the night large-amplitude group ($\tau = 20.1$ ms, $n = 4$, t -test, $P < 0.01$) and day large-amplitude group ($\tau = 21.5$ ms, $n = 10$; t -test, $P < 0.05$). Overall, the bimodal distribution of IA currents amplitudes observed in the dorsal SCN during the day and the difference in decay constants between small- and large-amplitude groups strongly suggest that there are two distinct populations of neurons in the SCN with functionally distinct IA channels and that these channels are regulated in a circadian manner.

DISCUSSION

In this study, we found that Kv4.1 and Kv4.2 channel subunits of the *Shal*-related family were expressed in the SCN, and electrophysiological analyses indicated that SCN neurons exhibit 4-AP sensitive IA currents that are active near resting membrane potentials. The physiological properties and pharmacological profiles of these IA currents in the SCN are similar to those previously reported from Kv4 channels (Jerng et al. 2004; Maffie and Rudy 2008). The magnitude of IA currents varied significantly across the circadian cycle, with larger currents recorded in dorsal SCN neurons during the daytime. This rhythm seems to be driven by a subset of SCN neurons expressing a larger peak current and a longer decay constant. Based on its biophysical properties as measured in SCN neurons along with its recorded properties in other CNS structures, the IA current is likely to have important roles in the regulation of spontaneous action potential firing of SCN neurons during the day and in the integration of synaptic inputs throughout the daily cycle.

Expression of the anatomical building blocks of the IA current, members of the Kv4 channel proteins and their transcripts, was shown in the SCN by Western blot and ISH (Figs. 1 and 2). The Kv4-family of K^+ channels is comprised of three distinct genes: Kv4.1, 4.2, and 4.3 (Birnbaum et al. 2004). The proteins encoded by these genes form tetramers of pore-forming subunits of the channels mediating the IA current (Isbrandt et al. 2000; Jerng et al. 2004; Maffie and Rudy 2008). Although a focus of this study was on expression of *Shal*-related family members, the Kv1.4 channel subunit has also been implicated in IA regulation and could be involved in the SCN. Interestingly, although expression of Kv4.2 has already been reported throughout the mammalian CNS (Coetzee et al. 1999), previous work has suggested that Kv4.1 is not prominently expressed within the brain (Serôdio and Rudy 1998). Not only did we find Kv4.1 expressed in the brain at both the transcript and protein levels in the mouse SCN, the ISH data (Fig. 1A) further suggests that the Kv4.1 subunit may be more widely distributed in the mammalian brain than previously believed.

This set of experiments raises the question of the functional roles played by the IA current generated by these Kv4 channels in SCN neurons. These neurons exhibit spontaneous rhythms in electrical activity with more activity in the day than night as well as have to process sensory inputs from the retina. As a field, we are interested in understanding the set of the ionic mechanisms responsible for these distinct processes. SCN neurons show a diurnal rhythm in membrane potential such that cells are depolarized by ~ 6 – 10 mV during the day compared with the night (Belle et al. 2009; de Jeu et al. 1998; Kuhlman and McMahon 2004). This day-night difference in resting membrane potential is largely mediated by a hyperpolarizing K^+ -dependent conductance that is sensitive to TEA: active at night at resting membrane potential and inactive during the day (Kuhlman and McMahon 2004, 2006). Our data indicate that IA is unlikely to be a major contributor to this K^+ driven daily rhythm in membrane potential. For one, the magnitude of the SCN IA current is completely insensitive to TEA, even at a 10 mM concentration (Fig. 4C), which is known to largely block the daily rhythm in V_m (Kuhlman and McMahon 2004). We did not study whether TEA altered the

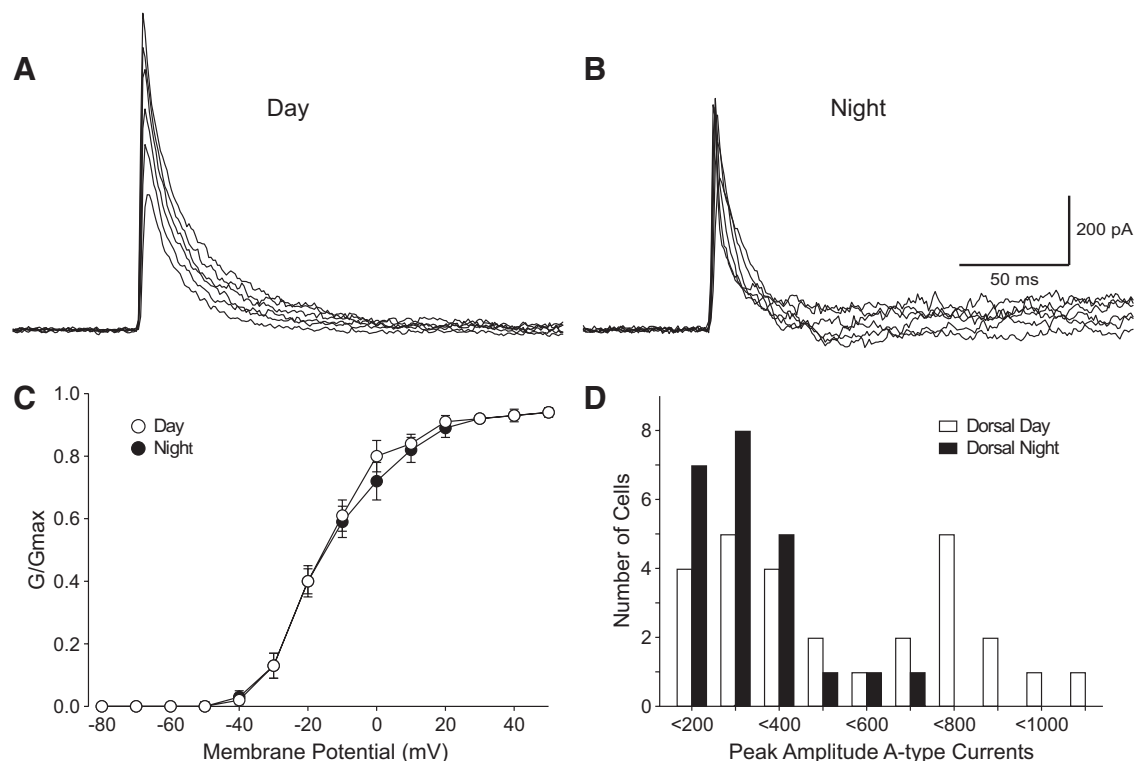


FIG. 6. Examples of largest magnitude IA current recorded in dorsal SCN in the day (A) and night (B). The activation curve did not change from day to night (C). Analysis of peak amplitude (D) indicates that a subset of cells with large amplitude IA currents are responsible for the peak during the day. During the night, dorsal SCN neurons exhibited IA currents that peaked between 100 and 400 pA. During the day, dorsal SCN neurons showed a bimodal amplitude distribution of maximal IA currents, with 1 peak found between 300 and 400 pA and another peak between 600 and 800 pA.

kinetics of the IA current, although previous work has found that TEA increases the inactivation time constant of IA in hamster SCN neurons (Alvado and Allen 2008). In addition, the IA current in the SCN peaks during the day and not the night (Fig. 5) as would be expected for the current driving the rhythm in resting membrane potential. The current we measured is maximally active in the SCN at membrane potentials between -45 and -55 mV (Fig. 3D), a voltage range correlated with a switch between the electrically active day and electrically silent night. Thus the IA current may well contribute to the day/night transitions in the membrane potential of SCN neurons.

Based on its voltage dependence and fast kinetics (Fig. 3), the IA should play a major role in determining whether a neuron will fire an action potential as well as aid in the repolarization of the membrane after an action potential is generated. During the day, SCN neurons generate regular patterns of action potentials with a frequency peaking between 5 and 10 Hz both in vitro (de Jeu et al. 1998; Herzog et al. 1998; Pennartz et al. 1998; Welsh et al. 1995) and in vivo (Meijer et al. 1998). The IA current is likely to play a role regulating this firing pattern (Bouskila and Dudek 1995) and be particularly important in tuning the higher firing rates. In a variety of other spontaneously active neurons, IA helps sculpt the pattern of action potentials during repetitive firing (Baranauskas 2007; Connor and Stevens 1971; Liss et al. 2001; Rudy 1988) that characterizes SCN neurons during the day. In a similar manner to the fast delayed rectifier (fDR) current (Itri et al. 2005), the IA could allow SCN neurons to discharge at higher rates during the day without adaptation. Furthermore,

the IA current has also been implicated in regulating the width of the action potential in hippocampal neurons (Kim et al. 2005), and spike width could have a major impact on secretion from the neurosecretory cells in the dorsal SCN region.

In addition to regulating membrane potential and action potential frequency, a third major function of intrinsic membrane currents is to regulate how neurons respond to synaptic input and, based on its biophysical properties, IA is likely to play a major role in synaptic integration within the SCN. Although SCN neurons are spontaneously active and generate rhythms in the absence of synaptic input, these neurons are embedded within a circuit and function within the context of this circuit. Even at resting conditions within the circuit, SCN neurons receive a low level glutamatergic (Michel et al. 2002) and a high level GABA-ergic synaptic input (Itri and Colwell 2003; Itri et al. 2004). Depending on the time of day and SCN region, these GABA_A-mediated inputs can evoke hyperpolarizing or depolarizing responses in the SCN neuron (Choi et al. 2008; Irwin and Allen 2009; Kim and Dudek 1992). During light exposure, the firing rate of SCN neurons is greatly increased with larger increases during the night than during the day (Meijer et al. 1998). These retinal-evoked excitatory postsynaptic responses in the SCN are mediated by AMPA (Cahill and Menaker 1989; Jiang et al. 1997; Kim and Dudek 1991; Michel et al. 2002) and N-methyl-D-aspartate (NMDA) receptors (Colwell 2001; Pennartz et al. 2001). These fast synaptic responses, whether mediated by AMPA or GABA_A receptors, exhibit a short time course and move the SCN neuron into a voltage range (Fig. 3) that would maximize the contribution of the IA current. In the hippocampus, several

studies suggest a role for the IA current in the regulation of dendritic excitability (Johnston et al. 2000; Kim et al. 2005, 2007). Similarly, in the olfactory bulb circuit, IA specifically regulates the dendritic inputs mediated by AMPA receptors (Schoppa and Westbrook 1999). Therefore based on our analysis of this current, we predict that IA will have a major role in determining how the SCN neuron responds to AMPA- and GABA-mediated signaling throughout the daily cycle.

In this study, we found that the magnitude of the IA current varied with the circadian cycle in at least a subset of SCN neurons. With this work, the IA current joins a handful of ionic currents that have been found to be regulated by the circadian system, including the fDR current (Itri et al. 2005), the L-type calcium current (Pennartz et al. 2002) and the calcium sensitive K^+ (BK) current (Pitts et al. 2006). The mechanisms responsible for circadian regulation are not well understood for any of the ionic currents studied to date. In the case of the fDR current, we have found evidence that the expression of the Kv3.1 and 3.2 channels that code for this current exhibit a daily rhythm. Interestingly, in cardiac tissue, diurnal variation in the expression of Kv4.2 has been described (Yamashita et al. 2003). However, in this study, we found that the expression of the Kv4 message (Fig. 1) and protein (Fig. 2) was stable between the day and night. Although our results were consistent for both the Kv4.1 and Kv4.2 message and protein in the SCN, we only sampled at two times, and more detailed analysis is needed before concluding that there is a complete lack of measurable rhythmicity. We feel that it is more likely that a circadian regulation of auxiliary proteins or posttranslational mechanisms is responsible for the observed circadian rhythm in the IA current. In the nervous system, Kv4 channels contain auxiliary proteins that function to modulate pore forming subunits (Maffie and Rudy 2008). These proteins are attractive targets for posttranslational regulation that could well mediate the daily rhythm in IA current that we observed in SCN neurons. Future studies will be needed to directly explore the mechanistic links between the molecular circadian oscillator and the Kv4 channels in the membrane of SCN neurons.

ACKNOWLEDGMENTS

We thank Drs. Kudo, Fulton, and Loh for comments on an early draft of this manuscript. We also thank D. Crandall for assistance with the graphics.

Present addresses: J. N. Itri, Department of Radiology, University of Pennsylvania, Philadelphia, PA 19104; J. M. Dragich, Department of Neurology, Columbia University, 650 West 168th St., New York, NY 10032; S. Michel, Department of Molecular Cell Biology, Leiden University Medical Center, PO Box 9600, 2300 RC Leiden, The Netherlands.

GRANTS

This work was supported by National Institutes of Health Grants MH-68087 to J. N. Itri; NS-63666 to A. M. Vosko; NS-058280 to A. Schroeder; NS-07101 to J. M. Dragich, and HL-084240 and NS-043169 to C. S. Colwell.

REFERENCES

Albus H, Bonnefont X, Chaves I, Yasui A, Doczy J, van der Horst GT, Meijer JH. Cryptochrome-deficient mice lack circadian electrical activity in the suprachiasmatic nuclei. *Curr Biol* 12: 1130–1133, 2002.

Alvado L, Allen CN. Tetraethylammonium (TEA) increases the inactivation time constant of the transient K^+ current in suprachiasmatic nucleus neurons. *Brain Res* 1221: 24–29, 2008.

Antle MC, Silver R. Orchestrating time: arrangements of the brain circadian clock. *Trends Neurosci* 28: 145–151, 2005.

Baranaskas G. Ionic channel function in action potential generation: current perspective. *Mol Neurobiol* 35: 129–150, 2007.

Belle MDC, Diekmann CO, Forger DB, Piggins HD. Daily electrical silencing in the mammalian circadian clock. *Science* 326: 281–284, 2009.

Birnbaum SG, Varga AW, Yuan LL, Anderson AE, Sweatt JD, Schrader LA. Structure and function of Kv4-family transient potassium channels. *Physiol Rev* 84: 803–833, 2004.

Bouskila Y, Dudek FE. A rapidly activating type of outward rectifier K^+ current and A-current in rat suprachiasmatic nucleus neurons. *J Physiol* 488: 339–350, 1995.

Cahill GM, Menaker M. Effects of excitatory amino acid receptor antagonists and agonists on suprachiasmatic nucleus responses to retinohypothalamic tract volleys. *Brain Res* 479: 76–82, 1989.

Chaudhury D, Loh DH, Dragich J, Hagopian A, Colwell CS. Select cognitive deficits in vasoactive intestinal peptide deficient mice. *BMC Neurosci* 9: 63, 2008.

Choi HJ, Lee CJ, Schroeder A, Kim YS, Jung SH, Kim JS, Kim do Y, Son EJ, Han HC, Hong SK, Colwell CS, Kim YI. Excitatory actions of GABA in the suprachiasmatic nucleus. *J Neurosci* 28: 5450–5459, 2008.

Coetzee WA, Amarillo Y, Chiu J, Chow A, Lau D, McCormack T, Moreno H, Nadal MS, Ozaita A, Poutney D, Saganich M, Vega-Saenz de Miera E, Rudy B. Molecular diversity of K^+ channels. *Ann NY Acad Sci* 868: 233–285, 1999.

Colwell CS. Circadian modulation of calcium levels in cells in the suprachiasmatic nucleus. *Eur J Neurosci* 12: 571–576, 2000.

Colwell CS. NMDA-evoked currents and calcium transients in the suprachiasmatic nucleus: gating by the circadian system. *Eur J Neurosci* 13: 1420–1428, 2001.

Colwell CS, Michel S, Itri J, Rodriguez W, Tam J, Lelievre V, Hu Z, Liu X, Waschek JA. Disrupted circadian rhythms in VIP- and PHI-deficient mice. *Am J Physiol Regul Integr Comp Physiol* 285: R939–R949, 2003.

Colwell CS, Michel S, Itri J, Rodriguez W, Tam J, Lelievre V, Hu Z, Waschek JA. Selective deficits in the circadian light response in mice lacking PACAP. *Am J Physiol Regul Integr Comp Physiol* 287: R1194–R1201, 2004.

Connor JA, Stevens CF. Inward and delayed outward membrane currents in isolated neural somata under voltage clamp. *J Physiol* 213: 1–19, 1971.

de Jeu M, Hermes M, Pennartz C. Circadian modulation of membrane properties in slices of rat suprachiasmatic nucleus. *Neuroreport* 9: 3725–3729, 1998.

Herzog ED, Takahashi JS, Block GD. Clock controls circadian period in isolated suprachiasmatic nucleus neurons. *Nat Neurosci* 1: 708–713, 1998.

Honma S, Shirakawa T, Katsuno Y, Namihira M, Honma K. Circadian periods of single suprachiasmatic neurons in rats. *Neurosci Lett* 250: 157–160, 1998.

Huang RC. Sodium and calcium currents in acutely dissociated neurons from rat suprachiasmatic nucleus. *J Neurophysiol* 70: 1692–1703, 1993.

Irwin RP, Allen CN. Calcium response to retinohypothalamic tract synaptic transmission in suprachiasmatic nucleus neurons. *J Neurosci* 27: 11748–11757, 2007.

Irwin RP, Allen CN. GABAergic signaling induces divergent neuronal Ca^{2+} responses in the suprachiasmatic nucleus network. *Eur J Neurosci* 30: 1462–1475, 2009.

Isbrandt D, Leicher T, Waldschütz R, Zhu X, Luhmann U, Michel U, Sauter K, Pongs O. Gene structures and expression profiles of three human KCND (Kv4) potassium channels mediating A-type currents I(TO) and I(SA). *Genomics* 64: 144–154, 2000.

Itri J, Colwell CS. Regulation of inhibitory synaptic transmission by vasoactive intestinal peptide (VIP) in the mouse suprachiasmatic nucleus. *J Neurophysiol* 90: 1589–1597, 2003.

Itri J, Michel S, Waschek JA, Colwell CS. Circadian rhythm in inhibitory synaptic transmission in the mouse suprachiasmatic nucleus. *J Neurophysiol* 92: 311–319, 2004.

Itri JN, Michel S, Vansteensel MJ, Meijer JH, Colwell CS. Fast delayed rectifier potassium current required for circadian neural activity. *Nat Neurosci* 8: 650–656, 2005.

Jackson AC, Yao GL, Bean BP. Mechanism of spontaneous firing in dorsomedial suprachiasmatic nucleus neurons. *J Neurosci* 24: 7985–7998, 2004.

Jerng HH, Pfaffinger PJ, Covarrubias M. Molecular physiology and modulation of somatodendritic A-type potassium channels. *Mol Cell Neurosci* 27: 343–369, 2004.

Jiang ZG, Yang Y, Liu ZP, Allen CN. Membrane properties and synaptic inputs of suprachiasmatic nucleus neurons in rat brain slices. *J Physiol* 499: 141–159, 1997.

- Johnston D, Hoffman DA, Magee JC, Poolos NP, Watanabe S, Colbert CM, Migliore M.** Dendritic potassium channels in hippocampal pyramidal neurons. *J Physiol* 525: 75–81, 2000.
- Kim J, Jung SC, Clemens AM, Petralia RS, Hoffman DA.** Regulation of dendritic excitability by activity-dependent trafficking of the A-type K⁺ channel subunit Kv4.2 in hippocampal neurons. *Neuron* 54: 933–947, 2007.
- Kim J, Wei DS, Hoffman DA.** Kv4 potassium channel subunits control action potential repolarization and frequency-dependent broadening in rat hippocampal CA1 pyramidal neurons. *J Physiol* 569: 41–57, 2005.
- Kim YI, Dudek FE.** Intracellular electrophysiological study of suprachiasmatic nucleus neurons in rodents: excitatory synaptic mechanisms. *J Physiol* 444: 269–287, 1991.
- Kim YI, Dudek FE.** Intracellular electrophysiological study of suprachiasmatic nucleus neurons in rodents: inhibitory synaptic mechanisms. *J Physiol* 458: 247–260, 1992.
- Ko CH, Takahashi JS.** Molecular components of the mammalian circadian clock. *Hum Mol Genet* 15: R271–R277, 2006.
- Ko GY, Shi L, Ko ML.** Circadian regulation of ion channels and their functions. *J Neurochem* 110: 1150–1169, 2009.
- Kuhlman SJ, McMahon DG.** Rhythmic regulation of membrane potential and potassium current persists in SCN neurons in the absence of environmental input. *Eur J Neurosci* 20: 1113–1117, 2004.
- Kuhlman SJ, McMahon DG.** Encoding the ins and outs of circadian pacemaker. *J Biol Rhythms* 21: 470–481, 2006.
- Liss B, Franz O, Sewing S, Bruns R, Neuhoff H, Roeper J.** Tuning pacemaker frequency of individual dopaminergic neurons by Kv4.3L and KChip3.1 transcription. *EMBO J* 20: 5715–5724, 2001.
- Maffie J, Rudy B.** Weighing the evidence for a ternary protein complex mediating A-type K⁺ currents in neurons. *J Physiol* 586: 5609–5623, 2008.
- Meijer JH, Watanabe K, Schaap J, Albus H, D t ari L.** Light responsiveness of the suprachiasmatic nucleus: long-term multiunit and single-unit recordings in freely moving rats. *J Neurosci* 18: 9078–9087, 1998.
- Michel S, Clark JP, Ding JM, Colwell CS.** BDNF and neurotrophin receptors modulate glutamate-induced phase shifts of the suprachiasmatic nucleus. *Eur J Neurosci* 24: 1109–1116, 2006.
- Michel S, Itri J, Colwell CS.** Excitatory mechanisms in the suprachiasmatic nucleus: the role of AMPA/KA glutamate receptors. *J Neurophysiol* 88: 817–828, 2002.
- Morin LP.** SCN organization reconsidered. *J Biol Rhythms* 22: 3–13, 2007.
- Pennartz CM, de Jeu MT, Bos NP, Schaap J, Geurtsen AM.** Diurnal modulation of pacemaker potentials and calcium current in the mammalian circadian clock. *Nature* 416: 286–290, 2002.
- Pennartz CM, De Jeu MT, Geurtsen AM, Sluiter AA, Hermes ML.** Electrophysiological and morphological heterogeneity of neurons in slices of rat suprachiasmatic nucleus. *J Physiol* 506: 775–793, 1998.
- Pennartz CM, Hamstra R, Geurtsen AM.** Enhanced NMDA receptor activity in retinal inputs to the rat suprachiasmatic nucleus during the subjective night. *J Physiol* 532: 181–194, 2001.
- Pitts GR, Ohta H, McMahon DG.** Daily rhythmicity of large-conductance Ca²⁺-activated K⁺ currents in suprachiasmatic nucleus neurons. *Brain Res* 1071: 54–62, 2006.
- Reppert SM, Weaver DR.** Coordination of circadian timing in mammals. *Nature* 418: 935–941, 2002.
- Rudy B.** Diversity and ubiquity of K channels. *Neurosci* 25: 729–749, 1988.
- Schaap J, Pennartz CM, Meijer JH.** Electrophysiology of the circadian pacemaker in mammals. *Chronobiol Int* 20: 171–188, 2003.
- Schoppa NE, Westbrook GL.** Regulation of synaptic timing in the olfactory bulb by an A-type potassium current. *Nat Neurosci* 2: 1106–1113, 1999.
- Schwartz WJ, Gross RA, Morton MT.** The suprachiasmatic nuclei contain a tetrodotoxin-resistant circadian pacemaker. *Proc Natl Acad Sci USA* 84: 1694–1698, 1987.
- Ser dio P, Rudy B.** Differential expression of Kv4 K⁺ channel subunits mediating subthreshold transient K⁺ (A-type) currents in rat brain. *J Neurophysiol* 79: 1081–1091, 1998.
- Wang LMC, Dragich JM, Kudo T, Odom IH, Welsh DK, O'Dell TJ, Colwell CS.** Expression of the circadian clock gene *Period2* in the hippocampus: possible implications for synaptic plasticity and learned behavior. *ASN Neuro* 1: 139–152, 2009.
- Welsh DK, Logothetis DE, Meister M, Reppert SM.** Individual neurons dissociated from rat suprachiasmatic nucleus express independently phased circadian firing rhythms. *Neuron* 14: 697–706, 1995.
- Yamaguchi S, Isejima H, Matsuo T, Okura R, Yagita K, Kobayashi M, Okamura H.** Synchronization of cellular clocks in the suprachiasmatic nucleus. *Science* 302: 1408–1412, 2003.
- Yamashita T, Sekiguchi A, Iwasaki YK, Sagara K, Inuma H, Hatano S, Fu LT, Watanabe H.** Circadian variation of cardiac K⁺ channel gene expression. *Circulation* 107: 1917–1922, 2003.